

Analysis of Cracks on a Fractured Surface of the Vehicle Crankshaft Using the Finite Element Method

Husaini*, T.E. Putra, Zulfikar

Laboratory of Computational Mechanics
Department of Mechanical Engineering – Universitas Syiah Kuala
Darussalam 23111 – Banda Aceh, Indonesia
*Corresponding author E-mail: husainifim@unsyiah.ac.id

Abstract

The purpose of this study is to determine the cause of fracture of a crankshaft. From visual examination, there was a beach mark on the surface, which is common in fatigue failure due to dynamic load. From the chemical composition testing, it was found that the material is classified into alloy steel. Hardness values of the material are based on the Rockwell method, which account the difference between the hardness values on the sides of the edge with the hardness in the middle part. The highest hardness value occurred on the outer edge of the cross section of the crankshaft on the X and Y axes at points 1 and 14, which was 102.2 HRB. A finite element analysis was performed to find out the values of stress, strain and deformation that occurred on the component of the crankshaft while operating. From these results, maximum stress and strain occur in the crank pin radius number 1. Finally, it can be concluded that fractures in the crankshaft occur for several reasons including fatigue failure, material hardness that is not in accordance with the standard, and initial cracks found in the radius of the area crank pin number 1.

Keywords: Finite Element Method, Fatigue Fracture, Crankshaft, Stress, Strain.

1. Introduction

Crankshaft is one of the main components of piston engine, which forwards the rotation of the connecting rod to the clutch. In turbo diesel engines, the increase in engine power tends to be observable. This usually leads to a decrease in engine component life [1]. Cracks generally start from the initial cracks that usually occur on the surface of weak material or in stress concentration areas, such as scratches and holes which results from repeated loading. This initial crack develops to a micro crack or propagation that forms a macro crack that culminates in failure [2]. Failure is a condition that causes the loss directly, usually caused by design errors, material defects, and maintenance errors [3,4].

Failure analysis is a process to determine the factors that cause loss of function of a component. It has been performed on crank-

shaft in several studies, such as by Lucjan Witek [5]. In the study, failure occurred on the crank pin number 2 after traveling a distance of 260,000 km. In 2016, M. Fonte [6] found that failure occurred on the crank pin number 3 after three years and 5000 hours of maintenance.

Many researchers concluded that most of the fatigue failures are due to dynamic loading [7,8]. To avoid failure of the crankshaft,

mistakes during disassembly and maintenance shall be avoided. Scratches, for example, will cause an initial flaw that will lead to failure. Failure usually starts from a critical point experiencing a high stress concentration as in the radius section and crank pin mounting errors [7]. Therefore, the purpose of this study is

to determine the cause of fracture in a crankshaft. Figure 1 shows the crankshaft parts.

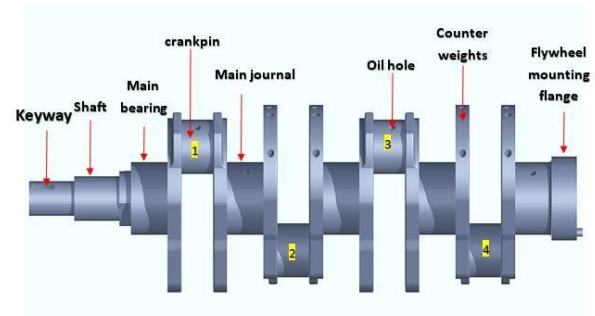


Fig. 1: The part of crankshaft.

2. Experimental Method

The type of the gasoline engine was machine F 10 A SOHC, 4 cylinder in line. This machine has 970 cc piston displacement, 1000 cc cylinder contents with maximum power of 7.5 Kgm / 3500 rpm and maximum torque of 50 Ps / 5500 rpm. Analysis was carried out on crankshaft failure by conducting visual inspection on the surface and using scanning electron microscopy (SEM) observations and microstructure and also testing the hardness value on the crankshaft. Furthermore, finite element analysis is carried out to determine the value of stress, strain and stress intensity factors that cause failure.

2.1. Material and visual inspection

In this study, the material used was alloy steel taken from the car crankshaft. First, observations were made to determine the mechanical properties of the material. The visual inspection showed a crack on the crankshaft with the engine rotation speed of 5500 RPM [9]. The crankshaft broken on crank pin number 1, as shown in Fig.ure 2. The visual inspection showed a beach mark on the fracture surface [10], as shown in Fig.ure 3, characterizing the cause of the failure.



Fig. 2: The failure of the crankshaft.

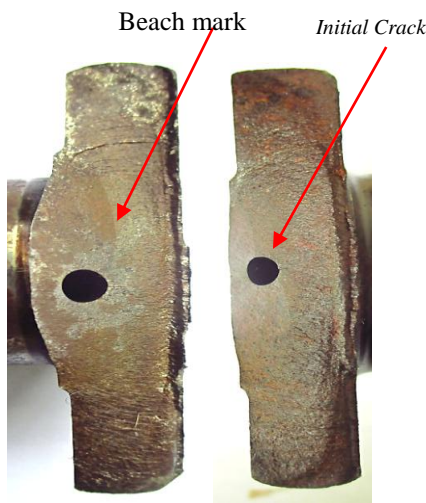


Fig. 3: The surface is broken on the crankshaft at the crank pin number 1.

Chemical composition examination was performed using a PDA-700 spectrometer to determine the elements contained in the material. Then, hardness testing was performed using Rockwell Type Zwick / Roell ZHR to determine the hardness value of the material, referring to ISO 6568 and ASTM 18 standard with load at the testing time of 100 kgf [11]. The tool also provided several holder for testing specimens with different dimensions such as cylinder and sphere. The experiments were performed on 14 different points using a 1/16 indenter ball. Microstructure testing was also performed using optical microscope Olympus GX 71 to view micro sized objects and make certain the grain boundaries and the properties of crankshaft material with 5 times to 100 times magnification. Finally, SEM observation was performed to see the broken surface on the crankshaft. The experimental testing was necessary to determine whether the initial cracks on the crankshaft resulted in failure.

2.2. Chemical Composition Testing

Table 1 shows the chemical composition of the examination results. It was found that the material was alloy steel AISI 1060 (ASTM A519) [12]. Its mechanical properties is tabulated in Table 2.

Table 1: The chemical composition of the material

Element	Spectroscopy results (%)	Chemical composition (AISI 1060) %
C	0,575	0,55 – 0,660
Mn	0,628	0,60 – 0,90
P	0,008	0,40 Max
S	0,025	0,050 Max

Table 2: Mechanical properties of AISI 1060 (ASTM A510)

Properties	Metric	Unit
Tensile strength (σ_B)	620	Mpa
Posion Ratio (V)	0.30	-
Density (ρ)	7850	Kg/m ³
Yield strength (σ_{ys})	485	MPa
Modulus young (E)	200	GPa
Shear modulus (S)	80	GPa
Hardness, Rockwell B	89	HRB
Fracture Toughness	36	MPa√m

2.3. Finite Element Analysis

Modeling

The crankshaft was modeled using a CAD software for analysis using finite element. Finite element analysis was performed to determine the stress, strain, deformation and stress intensity factor occurring on the crankshaft while operating. Figure 4 shows the crankshaft geometry that has been modeled. The geometry of the crankshaft was similar to the actual crankshaft size.

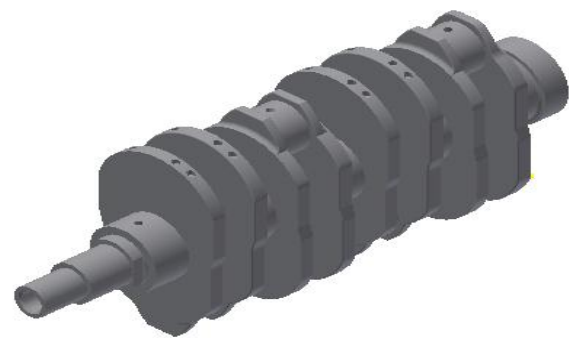


Fig. 4 : The geometry of the crankshaft.

Figure 5 shows the loading position on the crankshaft with a value of 1.5 MPa as shown in the yellow arrow. The ground on the middle of the axle is shown as red arrow. After applying the load, the next process was meshing to divide the model into smaller elements as it has a more significant effect on the accuracy, and can speed up the solution in elements [13]. The number of nodes obtained was 52,183 with the number of elements was 29,365. Figure 6 shows the meshing result 3D.

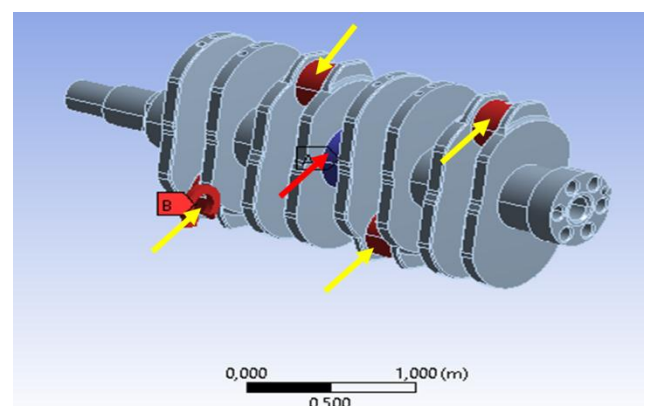


Fig. 5 : Loading on the crankshaft

After loading , meshing is performed to divide the parts of the crankshaft to small parts. Mesh in finite element analysis consists of three types of tetrahedrone, hexahedrone and triangle. In this research, the type of mesh used was tetrahedrone with mesh size 4 mm. The meshing of the crankshaft is shown in Fig.ure 6.

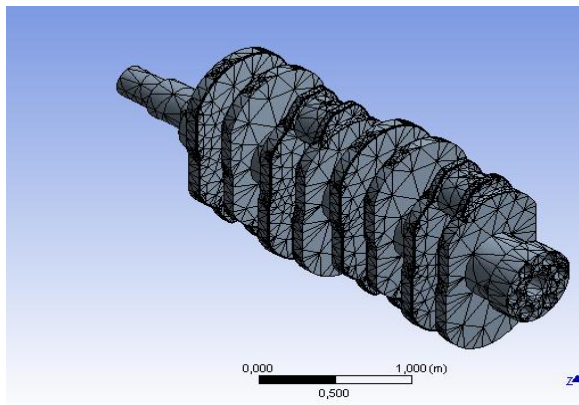


Fig. 6 : The Meshing of the crankshaft

3. Result and Discussion

3.1. Hardness test

From the hardness testing results, it was found that the highest hardness value was on the outer shell portion of the crankshaft on the X and Y axes at points 1 and 14, which were 102.2 HRB. The hardness testing point can be seen in Figure 7. Figure 8 shows that the highest hardness values are at points 1 and 14, which are at the edges of the cylindrical specimens as shown in Figure 7. The hardness of the shaft at the edges larger than the middle portion is aimed at avoiding defects and rapid thrust on the shaft during work.

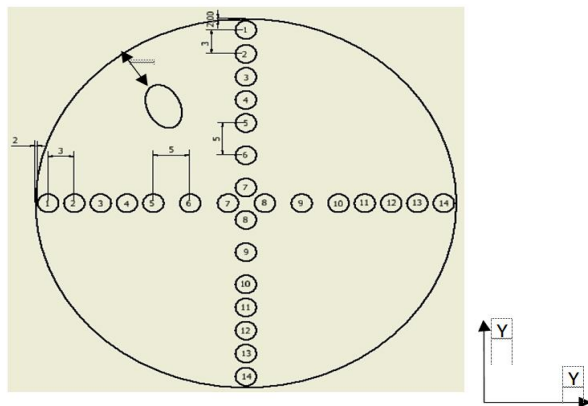


Fig. 7 : Hardness testing point

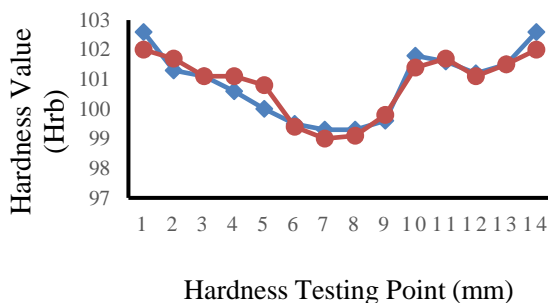


Fig. 8 : The graph of the hardness values (in HRB)

It was found that the hardness depth of about 13 mm from the outer surface of the crankshaft, namely from point 1 to 4 as shown in Figure 8, which also indicates the cause of failure. The heat treatment process was not suitable as the crankshaft was harder than the standard AISI 1060 material for approximately 89 HRB. Therefore, the hardness of the crankshaft was in excess of the standard, thus caused the fatigue failure.

3.2. SEM Observation

According to the SEM observation (SEM type EVO MA10), with enlargement of 3000x, there was a crack around oil hole on the crankshaft of pin 1 seen due to lack of care, negligence in the installation process, and a scratch with a sharp object resulting in the defect. The initial crack can be seen in Figure 9.

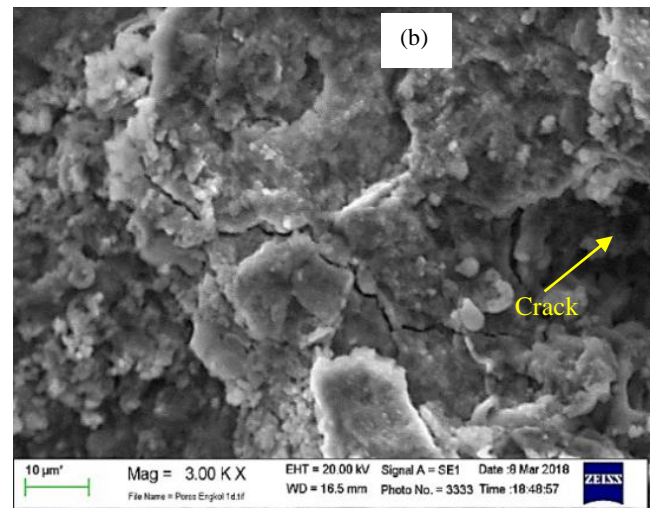
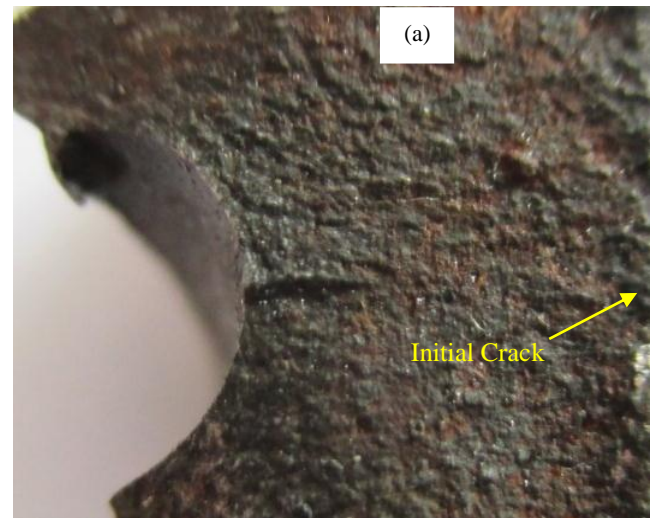


Fig. 9 : (a) Visual observation of the initial crack on the fracture surface and (b) SEM image on the fracture surface at the initial crack.

Observation of the factography using SEM as shown in Figure 9 shows the existence of the initial crack. However, the crankshaft remains a failure caused by the fatigue failure due to the dynamic loading through the beach mark on the crankshaft fracture surface that characterizes the fatigue failure as shown in Figure 3. Another cause was material hardness that was too deep by 13 mm from the outer surface of the crankshaft, making the crankshaft too hard and prone to fracture, as shown in Figure 8.

3.3. Microstructure

The microstructure test shows that the matrix was ferrite and pearlite with mean hardness value on x axis 100.85 and on y axis 100.83 HRB, showing that this material belongs to the steel hypoeutectoid, consisting of carbon content between 0.02-0.76% [14]. Figure 10 shows the results of microstructure testing with 20 times and 50 times magnification.

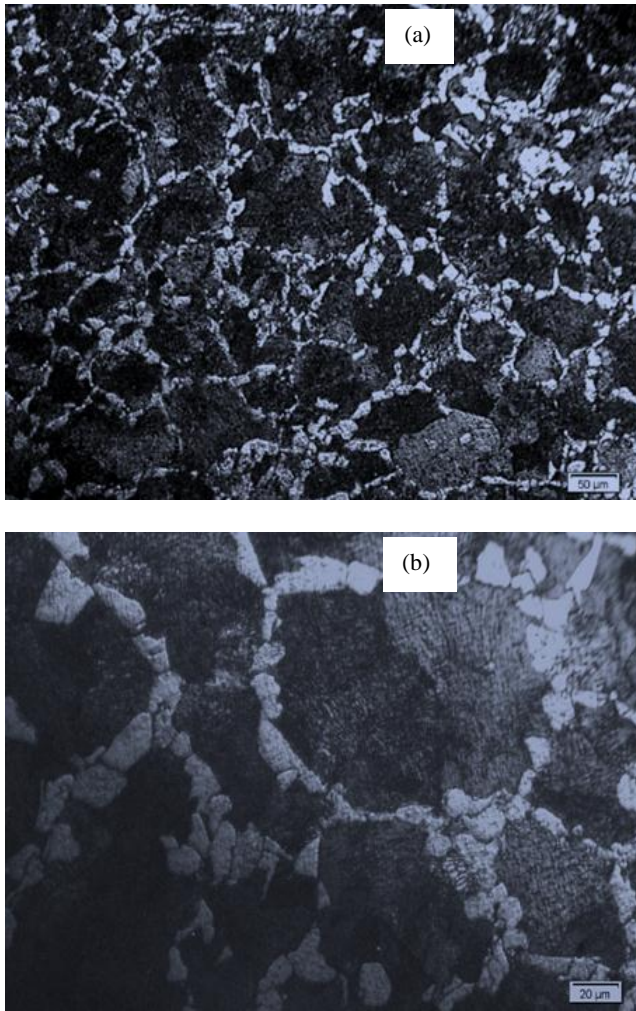


Fig. 10 : (a) The result of microstructure testing taken from the crankshaft (b) The result of the microstructure test taken from the crankshaft of magnification of the picture a.

3.4. Result of Finite Elements Analysis

The finite element analysis result shows that the maximum critical stress area was on the crank pin number 1, which was 98.235 MPa, especially in the radius of the crank pin due to the initial crack in the radius part of the crankshaft. Figure 11 shows the maximum equivalent stress result with the value of approximately 166 MPa.

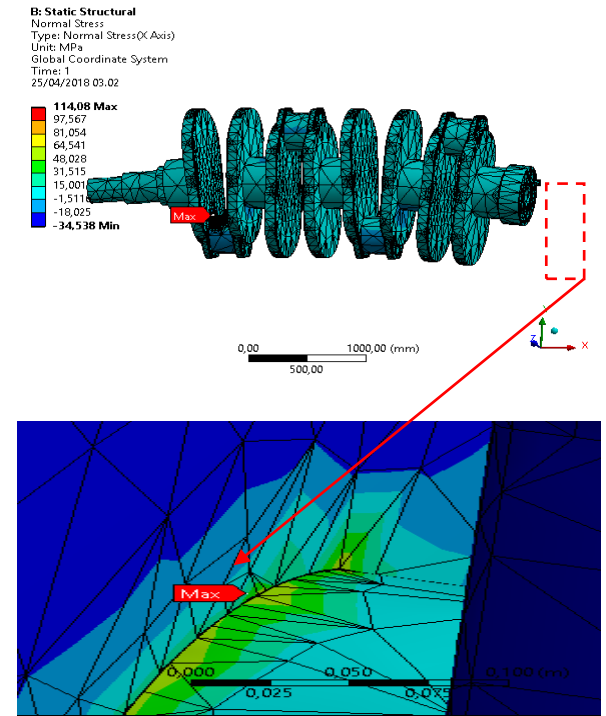


Fig. 11 : (a) Equivalent stress and (b) Enlargment at the maximum

Finite element analysis results show that the maximum strain value was 3892×10^{-3} caused by the initial crack in the radius of the crank pin, making it the most critical area when the load was applied as seen in Figure 12. The maximum deformation value was 2.952 mm, as shown in Figure 13.

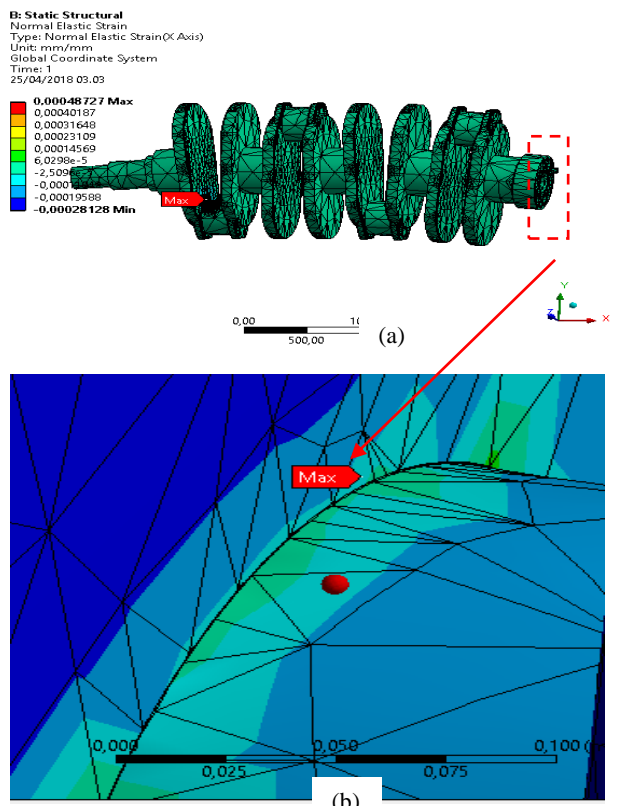


Fig. 12 : (a) Equivalent strain and (b) Enlargment at the maximum

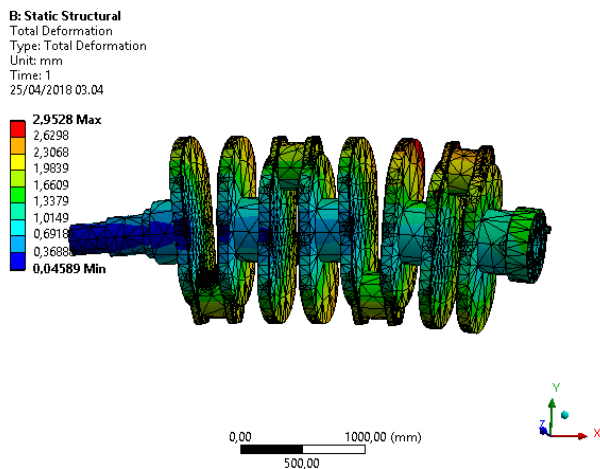


Fig. 13 : Deformasi

After SEM observation and observation of the crack, element analysis was done to determine the value of the maximum stress intensity factor that occurs on the crankshaft, which was 4.6 MPa $\sqrt{\text{m}}$ with the given stress was obtained on finite element analysis. Figure 14 shows the value of the stress intensity factor.

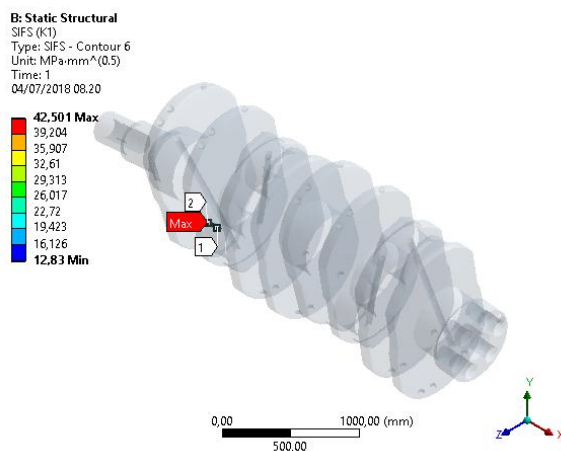


Fig. 14 : The value of maximum stress intensity factor

4. Conclusion

In this research, a series of investigations and analysis have been done from visual observation, observation with SEM, on broken surface and also finite element analysis to determine stress, strain and also stress intensity factor around the crack tip on crankshaft failure. The results of the cause of the failure on the crankshaft result in several conclusions:

1. From the visual analysis and also the observation with SEM, a fine crack which is the initial crack around the oil hole on the crankshaft of the crank pin number 1 was found.
2. On the surface of the fracture, the beach mark indicating that there has been a fatigue crack propagation causing fatigue failure was visible.
3. From finite element analysis, it was found that the maximum stress and strain occur on crank pin number 1.
4. The highest hardness value occurred at the outer edge of the crankshaft, which was 102 HRB. While still being close to 99 HRB, this is still not in accordance with the standard of material AISI 1060, which is 89 HRB, and this caused the failure.

Acknowledgement

The authors would like to express their gratitude to Universitas Syiah Kuala for financial support for this research through the grant No. 03/UN11.2/PP/PNBP/SP3/2018.

References

- [1] L. Witek, "Failure and thermo-mechanical stress analysis of the exhaust valve of diesel engine", *Engineering Failure Analysis*, Vol 66 (2016), pp:154-165.
- [2] Husaini, Zuhaimi, "Mixed mode fracture behavior of an aluminum alloy a6061 investigated by using compact tension shear specimens" *International Journal Of Technology (Ijtech)*, Vol 3 (2016), pp: 456-462,
- [3] Husaini, K. Kishimoto, M. Hanji, M. Notomi, "Investigations of the mixed mode crack growth behavior of an aluminum alloy" *ARPJ, Journal of Engineering and Applied Sciences*, Vol 2 (2016), pp: 885-889.
- [4] H. Akhyar, Husaini, Study on colling curve behavior during solidification and investigation of impact strength and hardness of Al-Zn aluminium alloy, *International journal of metal casting*, Vol 10 (2016), pp: 452-456.
- [5] L. Witek, M. Sikora, F. Stachowicz, T. Trzepiecinski, "Stress and failure analysis of the crankshaft of diesel engine", *Engineering Failure Analysis* Vol 82 (2017), pp:703 – 712 .
- [6] M. Fonte, V. Invante. M. Freitas, M. Reis, "failure mode analysis of two diesel engine crank,shaft", *Procedia Structural Integrity* Vol 1(2016), pp: 313–318 .
- [7] M. Fonte, V. Anes, P. Duarte, L. Reis, M. Freita, "Crankshaft failure analysis of a boxer diesel motor", *Engineering Failure Analysis* Vol 56(2015), pp:109-115.
- [8] T. E. Putra, S. Abdullah, D. Schramm, M. Z. Nuawi, T. Bruckmann, "Generating strain signals under consideration of road surface profiles", *Mechanical Systems and Signal Processing*, Vol 61(2015), pp: 485-497.
- [9] T. E. Putra, S. Abdullah, D. Schramm, M. Z. Nuawi, T. Bruckmann, "Reducing cyclic testing time for components of automotive suspension system utilising the wavelet transform and the Fuzzy C-Means", *Mechanical Systems and Signal Processing*, Vol 90 (2017), pp: 1-14.
- [10] Husaini, T. E. Putra, N. Ali, "Fatigue feature clustering of modified automotive strain signals for saving testing time", *International Journal of Automotive and Mechanical Engineering*, Vol 15 (2018) pp: 5251-5272.
- [11] ASTM E18-15, *Standart Test Method For Rockwell Hardness Of Metallic Materials* (ASTM International 2015)
- [12] ASTM A 519-9. *Standar Spesifikasi For Seamless Carbon And Alloysteel Mechanical Tubing*¹ (ASTM International. 2001).
- [13] F. J. Espadafor, J. B. Villanueva, M. T. Garcia "Analysis of a diesel generator crankshaft failure" *Engineering Failure Analysis* Vol 16 (2009), pp: 2333-2341.
- [14] Azom Materials. AISI 1060 *carbon steel* (UNS G51600), (2012).